

# Photolysis and oxidation by OH radicals of two carbonyl

## 2 nitrates: 4-nitrooxy-2-butanone and 5-nitrooxy-2-pentanone

Bénédicte Picquet-Varrault<sup>1</sup>, Ricardo Suarez-Bertoa<sup>2</sup>, Marius Duncianu<sup>3</sup>, Mathieu Cazaunau<sup>1</sup>,

4 Edouard Pangui<sup>1</sup>, Marc David<sup>1</sup>, Jean-François Doussin<sup>1</sup>

<sup>1</sup> LISA, UMR CNRS 7583, Université Paris-Est Créteil, Université de Paris, Institut Pierre Simon Laplace

6 (IPSL), Créteil, France

<sup>2</sup> European Commission Joint Research Centre (JRC), Ispra, Italy

8 <sup>3</sup> System Analyst Interscience BV, Brussels, Belgium

10 *Correspondence to:* B. Picquet-Varrault ([benedicte.picquet-varrault@lisa.u-pec.fr](mailto:benedicte.picquet-varrault@lisa.u-pec.fr))

### 12 Abstract

Multifunctional organic nitrates, including carbonyl nitrates, are important species formed in NO<sub>x</sub> rich atmospheres by the degradation of VOCs. These compounds have been shown to play a key role in the transport of reactive nitrogen and consequently in the ozone budget, but also to be important components of the total organic aerosol. However, very little is known about their reactivity in both gas and condensed phases. Following a previous study we published on the gas-phase reactivity of  $\alpha$ -nitrooxy ketones, the photolysis and the reaction with OH radicals of 4-nitrooxy-2-butanone and 5-nitrooxy-2-pentanone, respectively a  $\beta$ -nitrooxy ketone and a  $\gamma$ -nitrooxy ketone, were investigated for the first time in simulation chambers. The photolysis rates were directly measured in CESAM chamber which is equipped with a very realistic irradiation system. The ratios  $J_{\text{nitrate}}/J_{\text{NO}_2}$  were found to be  $(5.9 \pm 0.9) \times 10^{-3}$  for 4-nitrooxy-2-butanone and  $(3.2 \pm 0.9) \times 10^{-3}$  for 5-nitrooxy-2-pentanone under our experimental conditions. From these results, it was estimated that ambient photolysis frequencies calculated for 40° latitude North (1<sup>st</sup> July, noon) are  $(6.1 \pm 0.9) \times 10^{-5} \text{ s}^{-1}$  and  $(3.3 \pm 0.9) \times 10^{-5} \text{ s}^{-1}$  for 4-nitrooxy-2-butanone and 5-nitrooxy-2-pentanone, respectively. These results demonstrate that photolysis is a very efficient sink for these compounds with atmospheric lifetimes of few hours. They also suggest that, similarly to  $\alpha$ -nitrooxy ketones,  $\beta$ -nitrooxy ketones have enhanced UV absorption cross sections and quantum yields equal or close to unity and that  $\gamma$ -nitrooxy ketones have lower enhancement of cross sections which can easily be explained by the larger distance between the two chromophore groups. Thanks to a product study, branching ratio between the two possible photodissociation pathways are also proposed. Rate constants for the reaction with OH radicals were found to be  $(2.9 \pm 1.0) \times 10^{-12} \text{ cm}^3 \text{ molecule}^{-1} \text{ s}^{-1}$  and  $(3.3 \pm 0.9) \times 10^{-12} \text{ cm}^3 \text{ molecule}^{-1} \text{ s}^{-1}$ , respectively. These experimental data are in good agreement with rate constants estimated by the SAR of Kwok and Atkinson (1995) when using the parametrization proposed by Suarez-Bertoa et al. (2012) for carbonyl nitrates. Comparison with photolysis rates suggests that OH-initiated oxidation of carbonyl nitrates is a less efficient sink than photodissociation but is not negligible in polluted area.

## 1 Introduction

38 Organic nitrates play an important role as sinks or temporary reservoirs of NO<sub>x</sub>, as well as on ozone production  
40 in the atmosphere (Perring et al., 2013; Perring et al., 2010; Ito et al., 2007). They are formed by the degradation  
of VOCs in presence of NO<sub>x</sub> through two main processes: i) the reaction of peroxy radical, produced by the  
oxidation of VOCs, with NO. The major pathway is generally the reaction (1a) that leads to NO<sub>2</sub> formation. The  
42 reaction (1b) is a minor channel but it becomes gradually more important with increasing peroxy radical carbon  
chain length (Atkinson and Arey, 2003; Finlayson-Pitts and Pitts, 2000).



46 ii) The reaction of unsaturated VOCs with NO<sub>3</sub> radical, which proceeds mainly by addition of the nitrate radical  
on the double bond to produce nitro-alkyl radicals that can evolve into organic nitrates.

48 Among the organic nitrates, a variety of multifunctional species such as hydroxy-nitrates, carbonyl-nitrates and  
dinitrates are formed. The formed species have been shown to significantly contribute to the nitrogen budget in  
50 both rural and urban areas (Perring et al. 2013). Beaver et al. (2012) have observed that carbonyl nitrates, formed  
as second generation nitrates from isoprene, are an important fraction of the total organic nitrates observed over  
52 Sierra Nevada in summer. These observations are supported by several studies that investigated the  
photooxidation of isoprene in simulation chambers (Paulot et al., 2009, Müller et al., 2014). These  
54 multifunctional organic nitrates are also semi-/non-volatile and highly soluble species and are thus capable of  
partitioning into the atmospheric condensed phases (droplets, aerosols). Numerous field observations of the  
56 chemical composition of atmospheric particles have shown that organic nitrates represent a significant fraction  
(up to 75% in mass) of the total organic aerosol (OA) demonstrating that these species are important components  
58 of total OA (Ng et al., 2017).

Several modeling studies have also confirmed that multifunctional organic nitrates, in particular isoprene  
60 nitrates, play a key role in the transport of reactive nitrogen and consequently in the formation of ozone and  
other secondary pollutants at the regional and global scales (Horowitz et al., 2007; Mao et al., 2013; Squire et al.,  
62 2015). In particular, Mao et al. (2013) have performed simulations based on data from the ICARTT aircraft  
campaign across the eastern U.S. in 2004. They have shown that organic nitrates, which are mainly composed of  
64 secondary organic nitrates, including a large fraction of carbonyl nitrates, provide an important pathway for  
exporting NO<sub>x</sub> from the U.S.'s boundary layer, even exceeding the export of peroxy acyl nitrates (PANs).  
66 However, these modeling studies also point out the need for additional experimental data to better describe the  
sinks in both gas and condensed phases of multifunctional organic nitrates in models.

68 Recent experimental studies have revealed that hydrolysis in aerosol phase may be a very efficient sink of  
organic nitrates in the atmosphere (Bean and Hildebrand Ruiz, 2015; Rindelaub et al., 2015). These studies also  
70 suggest that the rate of these reactions strongly depends on the organic nitrate chemical structure and that  
additional work is needed to better understand these processes. In the gas-phase, photolysis and reaction with  
72 OH radical are expected to dominate the fate of organic nitrates (Roberts et al., 1990; Turberg et al., 1990). In a  
previous study, we have measured the photolysis frequencies and the rate constants for the OH-oxidation of 3

74 carbonyl nitrates ( $\alpha$ -nitrooxyacetone, 3-nitrooxy-2-butanone, and 3-methyl-3-nitrooxy-2-butanone) and we have  
shown that photolysis is the dominant sink for these compounds (Suarez-Bertoa et al., 2012). By comparison  
76 with absorption cross sections provided by Barnes et al. (1993), Müller et al. (2014) suggested i) that the  $\alpha$ -  
nitrooxy ketones have enhanced absorption cross sections, due to the interaction between the  $\text{-C=O}$  and  
78 the  $\text{-ONO}_2$  chromophore groups and ii) that the photolysis quantum yield is close to unity and  $\text{O-NO}_2$   
dissociation is the likely major channel. They also showed that this enhancement was larger at the higher  
80 wavelengths, where the absorption by the nitrate chromophore is very small. Therefore, they concluded that the  
absorption by the carbonyl chromophore was the one enhanced due to the neighbouring nitrate group.

82 These results are significant as they demonstrate that photolysis rates of these multifunctional species cannot be  
calculated as the sum of the monofunctional species (ketone + alkyl nitrate) ones. However, only  $\alpha$ -nitrooxy  
84 ketones were studied which leaves open the question of the persistence of the enhancement effect when the  
distance between the two functional groups increases. More recently, Xiong et al. (2016) have studied the  
86 atmospheric degradation (photolysis, OH-oxidation and ozonolysis) of *trans*-2-methyl-4-nitrooxy-2-buten-1-al  
(also called 4,1-isoprene nitrooxy enal) in order to better assess – as a model compound - the reactivity of  
88 carbonyl nitrates formed by the  $\text{NO}_3$ -initiated oxidation of isoprene. This compound has a conjugated  
chromophore  $\text{-C=C-C=O}$  in  $\beta$  position of the nitrate group. The authors measured the absorption cross sections  
90 of the nitroxy enal and compared them to those for the monofunctional species, i.e. methacrolein and isopropyl  
nitrate. They concluded that molecules containing  $\beta$ -nitrooxy ketones functionalities have also enhanced UV  
92 absorption cross sections. They also studied the kinetic and mechanisms for the oxidation of the nitroxy enal by  
OH and  $\text{O}_3$ . They conclude that photolysis and reaction with OH are thus the two main loss processes of *trans*-2-  
94 methyl-4-nitrooxy-2-buten-1-al, leading to a tropospheric lifetime of less than 1 h.

Given the large contribution of the carbonyl nitrates to the organic nitrate pool and the importance of their  
96 photochemistry for the  $\text{NO}_x$  budget, we present a study that aims at providing new experimental data on the gas-  
phase reactivity of these compounds. The study also seeks to disclose how photolysis and reaction with OH  
98 radical of carbonyl nitrates are affected by modifying their carbon chain length and the position of the two  
functional groups present in their molecular structure. Here, we provide the first photolysis frequencies and also  
100 the first rate constants for the OH-oxidation of two carbonyl nitrates: 4-nitrooxy-2-butanone and 5-nitrooxy-2-  
pentanone.

## 102 **2 Experimental section**

### **2.1 Reactants syntheses**

104 As a usual OH precursor in simulation chamber experiments, isopropyl nitrite was synthesized by dropwise  
addition of a dilute solution of  $\text{H}_2\text{SO}_4$  into a mixture of  $\text{NaNO}_2$  and isopropanol following the classical protocol  
106 proposed by Taylor et al. (1980).

On the contrary, 4-nitrooxy-2-butanone and 5-nitrooxy-2-pentanone were synthesized for the first time. A great  
108 care was taken to the development of a robust process: 4-nitrooxy-2-butanone and 5-nitrooxy-2-pentanone  
syntheses are based on Kames' method (Kames et al., 1993). This method consists in a liquid/gas phase reaction

110 where the corresponding hydroxy-ketone reacts with  $\text{NO}_3$  radicals released from the dissociation of  $\text{N}_2\text{O}_5$ .  $\text{N}_2\text{O}_5$   
112 was preliminarily synthesized in a vacuum line by reaction of  $\text{NO}_2$  with ozone, as described by Scarfoglio et  
114 al. (2006). The synthesis of the carbonyl nitrate is performed in a dedicated vacuum line connected to two bulbs,  
116 one containing the hydroxy-ketone, the other one containing  $\text{N}_2\text{O}_5$ . The two bulbs are also connected to each  
118 other. In a first step, the bulbs are placed in a liquid  $\text{N}_2$  cryogenic trap and pumped in order to remove air and  
120 impurities. In a second step, the cryogenic trap is removed from the bulb containing  $\text{N}_2\text{O}_5$  in order to let it warm  
122 and transfer into the bulb containing the hydroxy-ketone. Then, the bulb containing both reactants is stirred and  
kept at ice temperature for approximately 1h. Finally, the resulting carbonyl nitrate and nitric acid, its co-  
product, were separated by liquid-liquid extraction using dichloromethane and water. The carbonyl nitrate  
structure and purity were verified by FT-IR and GC-MS. Traces of impurities ( $\text{HCOOH}$  and  $\text{CH}_3\text{COOH}$ ) have  
been detected. The carbonyl nitrates were stored at  $-18^\circ\text{C}$  and under nitrogen atmosphere to prevent them from  
decomposition. Infrared spectra of 4-nitroso-2-butanone and 5-nitroso-2-pentanone are available on  
EUROCHAMP Data Centre (<https://data.eurochamp.org>).

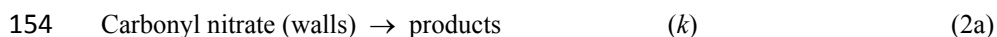
## 2.2 Determination of photolysis frequencies

124 The photolysis frequencies of the two carbonyl nitrates were determined by carrying out experiments in the  
CESAM simulation chamber which is only briefly described here as detailed information can be found in Wang  
126 et al. (2011). The chamber consists of a  $4.2\text{ m}^3$  stainless steel vessel equipped with a multiple reflection optical  
system interfaced to a FTIR spectrometer (Bruker Tensor 37) and also with  $\text{NO}$ ,  $\text{NO}_2$  and  $\text{O}_3$  analyzers (Horiba)  
128 to monitor the composition of the gas phase. The chamber is also equipped with three high pressure xenon arc  
lamps (MH-Diffusion, MacBeam 4000) which are combined with 7 mm Pyrex filters. This irradiation device  
130 provides a very realistic actinic flux (see comparison with the solar actinic flux in Figure S1) which allows  
measuring photolysis frequencies under realistic conditions (Wang et al., 2011; Suarez-Bertoa et al., 2012).  
132 However, since the intensity of the irradiation in CESAM chamber is lower than the one in ambient  
environment,  $J_{\text{nitrate}}/J_{\text{NO}_2}$  were provided in order to allow calculating  $J_{\text{nitrate}}$  under various sunlight conditions.  
134 Hence, the intensity of the actinic flux was determined by measuring the photolysis rate of  $\text{NO}_2$  ( $J_{\text{NO}_2}$ ) during  
dedicated experiments. 400 ppbv of  $\text{NO}_2$  in 1000 mbar of  $\text{N}_2$  were injected into CESAM chamber and kept in the  
136 dark for 20 min. The lights were then turned on during 20 min, and finally the mixture was left in the dark for an  
additional 20 min period. The photolysis frequency was subsequently determined using a kinetic numeric model  
138 developed for previous  $\text{NO}_x$  photo-oxidation experiments in CESAM (Wang et al., 2011). The fitting of  
modeled values from the measured data provided a  $\text{NO}_2$  photolysis frequency equal to  $2.2 \times 10^{-3}\text{ s}^{-1}$  ( $\pm 0.01, 2\sigma$   
140 error).

During a typical experiment, carbonyl nitrates were introduced into the chamber which was preliminarily filled  
142 at atmospheric pressure with  $\text{N}_2/\text{O}_2$  (80/20). For the injection, the bulb containing the carbonyl nitrate was  
connected to the chamber and slightly heated while it was flushed with  $\text{N}_2$ . Mixing ratios of carbonyl nitrates  
144 ranged from hundreds ppb to ppm. Because carbonyl nitrates may decompose during the injection, large amounts  
of  $\text{NO}_2$  (hundreds ppb) were present in the mixture. Cyclohexane was also added to the mixture as an OH-  
146 scavenger with mixing ratios of approx. 4 ppm. Considering the fact that cyclohexane is approximately twice  
more reactive with OH radicals than the carbonyl nitrates (see Results section), it was estimated that between 80  
148 and 98% of the OH radicals were scavenged (depending on the experiment considered). The mixture was kept

under dark conditions during two hours to be able to assess the impact of the reactor's walls and to minimize their effects by passivation. Then, the mixture was irradiated during 3 hours. For most experiments, the mixture was finally left in the dark for approximately 1 hour after the irradiation period to allow for verifying if wall losses were constant during the entire duration of the experiment.

During the experiment, the carbonyl nitrate loss processes can be described as:



$$-\frac{d[\text{nitrate}]}{dt} = (J_{\text{nitrate}} + k) \times [\text{nitrate}] \quad (\text{Eq. 1})$$

$$\ln[\text{nitrate}]_t = \ln[\text{nitrate}]_0 - (k + J_{\text{nitrate}}) \times t \quad (\text{Eq. 2})$$

The reaction (2a) had to be added to the system to take into account the interaction or adsorption of the carbonyl nitrates on the stainless steel walls of CESAM during the experiments. By plotting  $\ln[\text{nitrate}]_t$  vs. time, where  $[\text{nitrate}]_t$  is the concentration of the carbonyl nitrate at time  $t$ , a straight line is obtained with a slope of  $(k + J_{\text{nitrate}})$ . The same approach was applied to each of the 'dark' periods, before and after irradiation, to determine their respective dark decay rates, namely  $k_{\text{before}}$  and  $k_{\text{after}}$  and  $k$  was calculated as the average of  $k_{\text{before}}$  and  $k_{\text{after}}$  for each experiment. Finally,  $J_{\text{nitrate}}$  was calculated as the difference between the loss rate during the irradiation period  $(k + J_{\text{nitrate}})$  and the averaged loss rate during the dark periods  $(k)$ .

The uncertainties were calculated by adding the respective statistical errors ( $2\sigma$ ) associated to the dark and light periods, the former set as the average of the uncertainties determined for both dark periods (i.e., before and after irradiation). However, for some experiments, it was observed that the dark decay rate before irradiation was significantly higher than the one after, suggesting that wall loss process is more complex than a "simple" first order process and may decrease with time due to a passivation of the walls. More generally, interactions of gases with walls remain poorly understood and are currently subject to intensive investigations by the scientific community. Here, in order to determine wall loss decays which are as representative as possible of the one during the irradiation period, the first experimental points (after the injection of the carbonyl nitrate) were not taken into account for the linear fit leading to the determination of  $k_{\text{before}}$ . In addition, the uncertainty was not calculated using the approach detailed above, the statistical error being too low compared to the difference between  $k_{\text{before}}$  and  $k_{\text{after}}$ . The uncertainty was thus estimated in order to include the lowest and the highest  $J_{\text{nitrate}}$  values calculated with the highest and the lowest  $k$  value, respectively. Finally, the overall uncertainty associated with the photolysis rate of each of the carbonyl nitrates was calculated as the average of the uncertainties obtained for each experiment, divided by the square root of the number of experiments (2 or 3).

### 2.3 Determination of the OH-oxidation rate constants

The kinetic experiments for the OH-oxidation of the carbonyl nitrates were performed in the CSA chamber at room temperature and atmospheric pressure, in a mixture of  $\text{N}_2/\text{O}_2$  (80/20). The chamber consists of a 977 L Pyrex<sup>TM</sup> vessel irradiated by two sets of 40 fluorescent tubes (Philips TL05 and TL03) that surround the chamber. The emissions of these black lamps are centered on 360 and 420 nm, respectively. The chamber is

184 equipped with a multiple reflection optical system with a path length of 180 m interfaced to a FTIR spectrometer  
(Vertex 80 from Bruker). Additional details about this smog chamber are given elsewhere (Doussin et al., 1997;  
186 Duncianu et al., 2017).

The relative rate technique was used to determine the rate constant for the OH-oxidation of the carbonyl nitrates  
188 with methanol as reference compound. We used the IUPAC recommended value  $k_{(\text{methanol}+\text{OH})} = (9.0 \pm 1.8) \times$   
 $10^{-13} \text{ cm}^3 \text{ molecule}^{-1} \text{ s}^{-1}$  (<http://www.iupac-kinetic.ch.cam.ac.uk/>). Hydroxyl radicals were generated by  
190 photolyzing isopropyl nitrite. Initial mixing ratios of reactants (carbonyl nitrate, isopropyl nitrite, methanol and  
NO) were in the ppm range. As previously described, the carbonyl nitrate was introduced into the chamber by  
192 connecting the bulb to the chamber and by slightly heating and flushing it with N<sub>2</sub>. NO was added to the mixture  
in order to enhance the formation of OH radicals by reaction with HO<sub>2</sub> radicals which are formed by isopropyl  
194 nitrite photolysis. All experiments were conducted during a 1 h period of continuous irradiation.

Prior to the experiments, it was verified that photolysis and wall losses of the studied compounds were negligible  
196 under our experimental conditions. This can be explained by the facts that i) the irradiation system of CSA  
chamber emits photons at significantly higher wavelengths than the one of CESAM chamber, and ii) the walls of  
198 the chamber are made of Pyrex which is more chemically inert than stainless steel. It was therefore assumed that  
reaction with OH is the only fate of both, the studied compound (carbonyl nitrate) and the reference compound  
200 (methanol) and that neither of these compounds is reformed at any stage during the experiment. Based on these  
hypotheses, it can be shown that (Atkinson, 1986):

$$202 \quad \ln \frac{[\text{nitrate}]_0}{[\text{nitrate}]_t} = \frac{k_{\text{nitrate}}}{k_{\text{methanol}}} \times \frac{[\text{methanol}]_0}{[\text{methanol}]_t} \quad (\text{Eq. 3})$$

where [nitrate]<sub>0</sub> and [methanol]<sub>0</sub>, and [nitrate]<sub>t</sub> and [methanol]<sub>t</sub> stand for the concentration of the carbonyl nitrate  
204 and the reference compound at times 0 and t, respectively. The plot  $\ln([\text{nitrate}]_0/[\text{nitrate}]_t)$  vs.  
 $\ln([\text{methanol}]_0/[\text{methanol}]_t)$  is linear with a slope equal to  $k_{\text{nitrate}}/k_{\text{methanol}}$  and an intercept of zero. The uncertainty  
206 on  $k_{\text{nitrate}}$  was calculated by adding the relative uncertainty corresponding to the statistical error on the linear  
regression ( $2\sigma$ ) and the error on the reference rate constant (here 20 % for methanol).

## 208 2.4 Chemicals and gases

Dry synthetic air was generated using N<sub>2</sub> (from liquid nitrogen evaporation, >99.995% pure, <5 ppm H<sub>2</sub>O, Linde  
210 Gas) and O<sub>2</sub> (quality N45, >99.995% pure, <5 ppm H<sub>2</sub>O, Air Liquide). Chemicals obtained from commercial  
sources are: NO (quality N20, >99% Air Liquide), NO<sub>2</sub> (quality N20, >99% Air Liquide), 4-hydroxy-2-butanone  
212 (95% Aldich), 5-hydroxy-2-pentanone (95% Aldich), cyclohexane (VWR), methanol (J.T. Baker), H<sub>2</sub>SO<sub>4</sub> (95%  
VWR), NaNO<sub>2</sub> (≥99 Prolabo), isopropanol (VWR).

## 214 3 Results and discussion

### 3.1 Photolysis of carbonyl nitrates

216 Figure 1 presents the kinetic plots obtained for the two compounds, where  $\ln[\text{nitrate}]$  was plotted as a function of  
time. A significant decrease was observed for both compounds during the dark period, before and after

218 irradiation, suggesting that they adsorb or decompose on the walls. Photolysis frequencies were thus calculated  
220 as the difference between the decay rates in the dark and the one under irradiation (see section 2.2). Results  
222 obtained for both compounds and for all experiments are given in Table 1. For 4-nitrooxy-2-butanone, photolysis  
224 frequencies are in good agreement despite the fact that decay rates in the dark differ from an experiment to  
226 another. For 5-nitrooxy-2-butanone, it can be seen that the decay rate in the dark before irradiation is  
significantly higher than the one after (in particular for experiments 3 and 4), suggesting that wall losses may  
decrease with time due to a passivation of the walls. Despite this, comparison of the three experiments showed  
good agreement. For CESAM irradiation conditions, the photolysis rates are  $(1.3 \pm 0.2) \times 10^{-5} \text{ s}^{-1}$  for 4-nitrooxy-  
2-butanone and  $(0.7 \pm 0.2) \times 10^{-5} \text{ s}^{-1}$  for 5-nitrooxy-2-pentanone. Hence,  $J_{\text{nitrate}}/J_{\text{NO}_2}$  were found to be  $(5.9 \pm 0.9)$   
 $\times 10^{-3}$  for 4-nitrooxy-2-butanone and  $(3.2 \pm 0.9) \times 10^{-3}$  for 5-nitrooxy-2-pentanone.

228 These photolysis rates have been compared in Table 2 to those we obtained in a previous study (Suarez-Bertoa et  
230 al., 2012) for 3-nitrooxy-2-propanone, 3-nitrooxy-2-butanone and 3-methyl-3-nitrooxy-2-butanone using the  
232 same experimental conditions and methodology. Experimental photolysis frequencies have also been compared  
234 to those calculated using cross sections published in the literature and by assuming a quantum yield equal to  
236 unity. The intensity of the actinic flux in CESAM chamber was determined by combining measurement of the  
spectrum of the lamps with a spectroradiometer and determination of  $J_{\text{NO}_2}$  by chemical actinometry (see section  
2.2). For 3-nitrooxy-2-propanone and 3-nitrooxy-2-butanone, cross sections were taken from Barnes et al.  
(1993). For 4-nitrooxy-2-butanone and 5-nitrooxy-2-pentanone, for which no data have been provided in the  
literature, cross sections were estimated using those for corresponding monofunctional species and by applying  
the enhancement factor ( $r_{nk}$ ) obtained for 3-nitrooxy-2-propanone (Müller et al., 2014):

$$238 \quad r_{nk} = \frac{s_{nk}}{s_n + s_k} \quad (\text{Eq.4})$$

Where  $s_{nk}$ ,  $s_n$  and  $s_k$  are the absorption cross sections of the keto nitrate, the alkyl nitrate and the ketone,  
240 respectively. For 4-nitrooxy-2-butanone, cross sections of 2-butanone and 1-butyl nitrate were taken from  
IUPAC, 2006. For 5-nitrooxy-2-pentanone, cross sections of 2-pentanone ([http://satellite.mpic.de/spectral\\_atlas](http://satellite.mpic.de/spectral_atlas))  
242 and 1-pentyl nitrate (Clemitshaw et al., 1997) were used. From these results, it can be observed that the  
244 experimental photolysis frequencies ( $J_{\text{exp}}$ ) obtained for 3-nitrooxy-2-propanone and 4-nitrooxy-2-butanone are  
very close and can be considered as equal within uncertainties. This suggests that the strong enhancement in the  
cross sections induced by the interaction between the two functional groups, which has been observed for  $\alpha$ -  
246 nitrooxy ketones, also exists with the same amplitude for  $\beta$ -nitrooxy ketones. This is confirmed by the fact the  
experimental value for 4-nitrooxy-2-butanone is in very good agreement with the calculated value, obtained by  
248 assuming that the enhancement factor is the same as the one for 3-nitrooxy-2-propanone. This effect,  
nonetheless, seems to fade away when the two functions are one carbon further away: The experimental  
250 photolysis frequency obtained for 5-nitrooxy-2-pentanone is indeed significantly lower than those for 3-  
nitrooxy-2-propanone and 4-nitrooxy-2-butanone. It is also much lower than the J value calculated by assuming  
252 the same enhancement factor as for 3-nitrooxy-2-propanone. This result suggests that the enhancement is  
significantly reduced for  $\gamma$ -nitrooxy ketones even if it is probably not totally absent. This can easily be explained  
254 by the fact that the inductive effect of the nitrate group is expected to decrease when the distance between the  
functional groups increases. Another explanation would be that the quantum yield is significantly lower than

256 unity. Finally, by comparing results for 3-nitrooxy-2-propanone, 3-nitrooxy-2-butanone and 3-methyl-3-  
258 nitrooxy-2-butanone, it can be observed that photolysis frequencies increase with the substitution of the alkyl  
chain. From these kinetic data, it can be concluded that photolysis frequencies of  $\alpha$ - and  $\beta$ -nitrooxy ketones are  
260 much higher than those obtained when considering the sum of the photolysis frequencies for monofunctional  
species.

Products formed by the photolysis of the carbonyl nitrates were investigated by FTIR spectrometry. For both  
262 compounds, only peroxy acetyl nitrate (PAN) was detected. To calculate its formation yield, concentration of  
PAN was plotted as a function of  $-\Delta[\text{nitrate}]_{\text{photolysis}}$ , i.e., the carbonyl nitrate loss rate due to photolysis. This one  
264 was calculated by subtracting the loss rate measured during the dark period before the photolysis to the one  
measured during the photolysis. Because the yield was calculated as the initial slope of the plot, it was  
266 considered that the dark period before irradiation was more representative than the one after. The uncertainty on  
the yield was calculated by taking into account the uncertainties on the infrared absorption cross sections of PAN  
268 (10%) and carbonyl nitrates (10%) as well as the uncertainty on  $J$  (see table 1). For 5-nitrooxy-2-pentanone, this  
uncertainty is quite large because the photolysis rate is relatively slow in comparison to loss to the reactor walls.  
270 PAN formation yields obtained for both compounds are given in Table 1.

For 4-nitrooxy-2-butanone, PAN is formed with a yield equal to unity. Its formation can be explained by the  
272 dissociation of the C(O)-C bond as shown in Scheme 1. This pathway also leads to the formation of the alkyl  
radical  $\cdot\text{CH}_2\text{-CH}_2\text{ONO}_2$  which reacts with  $\text{O}_2$  to form the corresponding peroxy radical, this latter evolving to the  
274 formation of the alkoxy by reaction with NO. Two pathways have been considered for the evolution of the  
alkoxy radical: i) the decomposition which may lead to the formation of  $\text{NO}_2$  and two molecules of HCHO and  
276 ii) the reaction with  $\text{O}_2$  which produces nitrooxy ethanal, also called ethanal nitrate ( $\text{CH}_2(\text{ONO}_2)\text{-CH(O)}$ ). None  
of these two products have been detected by FTIR. However, absorption bands of ethanal nitrate are expected to  
278 be very similar to those of the reactant and it may thus be difficult to distinguish them. In addition, ethanal  
nitrate is expected to photodissociate much faster than the keto nitrate. The other photodissociation pathway is  
280 the cleavage of the O- $\text{NO}_2$  bond. It leads to the formation of the radical  $\text{CH}_3\text{C(O)CH}_2\text{CH}_2\text{O}\cdot$  which is expected  
to react with  $\text{O}_2$  to form a dicarbonyl product. This product was not observed and this is in good agreement with  
282 the formation of PAN with a yield equal to unity by the other photodissociation pathway. It should be noticed  
that PAN has been detected as a primary product suggesting that its formation via the photolysis of the  
284 dicarbonyl product is not expected. In our experiments, it was not possible to measure  $\text{NO}_2$  formation yield  
because large amounts of  $\text{NO}_2$  (hundreds ppb) were introduced with the carbonyl nitrate (probably due to its  
286 decomposition during the injection).

As discussed above, since the enhancement in the cross sections is larger at the higher wavelengths, where  
288 absorption by the nitrate chromophore is very small, it was proposed by Müller et al. (2014) that the absorption  
by the carbonyl chromophore is enhanced due to the neighboring nitrate group. The authors also suggest that the  
290 photodissociation proceeds by a dissociation of the weak O- $\text{NO}_2$  bond, i.e. that a photon absorption by one  
chromophore (carbonyl group) causes dissociation in another part of the molecule (nitro group). This is not in  
292 line with what we observed in our study. From our experiments, we conclude that the photolysis of 4-nitrooxy-2-  
butanone proceeds mainly by a dissociation of the C(O)-C bond. In the former study on the photolysis of 3-  
294 nitrooxy-2-propanone, 3-nitrooxy-2-butanone and 3-methyl-3-nitrooxy-2-butanone (Suarez-Bertoa et al., 2012),



PAN and carbonyl compounds (respectively, formaldehyde, acetaldehyde and acetone) were detected as major products. However, branching ratio of the two pathways (dissociation of O-NO<sub>2</sub> and C(O)-C bonds) could not be determined as the formation of these products, in particular PAN, can be explained by the two pathways.

For 5-nitrooxy-2-pentanone, formation yield of PAN has been observed to be much lower:  $0.16 \pm 0.08$ . As for 4-nitrooxy-2-butanone, its formation can be explained by the dissociation of the C(O)-C bond (see Scheme 2). This result suggests that both dissociation pathways may occur and that O-NO<sub>2</sub> dissociation could be the major one. However, this was not confirmed by the detection of the dicarbonyl compound (2-oxo-pentanal) which is expected to be formed by this pathway. Despite the fact that no standard was available for this compound, no characteristic band was observed in the residual spectrum (after subtraction of reactants and PAN spectra). Because the photolysis rate of 5-nitrooxy-2-pentanone is very low, we suspect that the concentration of this product is below the detection limit. Nevertheless, the low PAN yield is a strong indication that O-NO<sub>2</sub> dissociation may be the major pathway, contrary to what has been observed for 4-nitrooxy-2-butanone. This should be considered in the light of the low enhancement of absorption cross sections which has been assumed for this compound. Hence, in the case of  $\gamma$ -nitrooxy ketones, the enhancement of the absorption by the carbonyl chromophore seems to significantly decrease, leading to a lower branching ratio of the C(O)-C bond dissociation.

### 3.2 OH-oxidation of carbonyl nitrates

Rate constants of the OH-oxidation have been measured for 4-nitrooxy-2-butanone and 5-nitrooxy-2-pentanone. Prior to the experiments, it was checked that the carbonyl nitrates do not photolyse nor decompose/adsorb on the walls of the chamber. Figure 2 represents the kinetic plots obtained for the two carbonyl nitrates. For each compound, several independent kinetic experiments were performed and data were combined to provide the  $k_{\text{ketonitrate}}/k_{\text{methanol}}$  for each compound (see Figure 3). In order to limit errors in the quantification of reactants due to the possible formation of carbonyl nitrates as products, only the very beginning of the experiments was taken into account for the kinetic plots. This explains the small number of experimental points. The obtained rate constants are given in Table 3. These data are, to our knowledge, the first determinations of the rate constants for the reaction of OH with these two carbonyl nitrates. From these data, it can be concluded that 4-nitrooxy-2-butanone and 5-nitrooxy-5-pentanone have similar reactivity towards OH radicals with rate constants equal to  $(2.9 \pm 1.0) \times 10^{-12}$  and  $(3.3 \pm 0.9) \times 10^{-12}$  cm<sup>3</sup> molecule<sup>-1</sup> s<sup>-1</sup>, respectively.

Rate constants provided in this study, as well as those previously reported for a series of  $\alpha$ -nitrooxy-ketones (Suarez-Bertoa et al., 2012) have been compared to those estimated using structure-activity relationships (SARs) in Table 4. Different SARs have been evaluated: i) the one developed by Kwok and Atkinson (1995) with updated factors  $F(-\text{ONO}_2) = 0.14$  and  $F(-\text{C-ONO}_2) = 0.28$  from Bedjanian et al. (2018); ii) the one developed by Kwok and Atkinson (1995) with updated factors  $F(-\text{ONO}_2) = 0.8$  and  $F(-\text{C-ONO}_2) = 0.1$  from Suarez-Bertoa et al. (2012); iii) the one developed by Neeb (2000) which proposes a different type of parametrization and has been observed to be particularly accurate for oxygenated species; and iv) the one developed by Jenkin et al. (2018) which proposes a parametrization very similar to the one from Kwok and Atkinson (1995) and Bedjanian et al. (2018). The rate constant for 5-nitrooxy-2-pentanone is reasonably well reproduced by all SARs (within a factor of 2). For 4-nitrooxy-2-butanone, only the parametrization provided by Suarez-Bertoa et al. (2012)

succeeds in reproducing the experimental value. This can be explained by the fact that this parametrization has been optimized for carbonyl nitrates while the others have been developed using the entire dataset for compounds containing a nitrate group (-ONO<sub>2</sub>) (Jenkin et al., 2018) or using the dataset for alkyl nitrates (Bedjanian et al., 2018). The main difference between these parametrizations is that in Suarez-Bertoa et al. (2012), the factor F(-ONO<sub>2</sub>) is much less deactivating than for the others. This could result from electronic interactions between the two functional groups. However, Suarez-Bertoa et al. (2012) noticed that their parametrization gives poor results for alkyl nitrates, suggesting that a specific parametrization has to be used for multifunctional species. This also suggests that the principle of SARs based on the group additivity method may not be suitable for multifunctional molecules.

From these experiments, several oxidation products have been detected: HCHO, PAN and methylglyoxal for 4-nitrooxy-2-butanone, and HCHO, PAN and 3-nitrooxy-propanal for 5-nitrooxy-2-pentanone. However, their quantification was highly uncertain because the infrared spectra were complex due to the presence of methanol, isopropyl nitrite, impurities (in particular acetic acid) and their oxidation products. Dedicated mechanistic experiments should now/in the near future be performed using HONO as OH source in order to simplify the chemical mixture.

### 3.3 Atmospheric implications

Atmospheric lifetimes of the investigated compounds are presented in Table 5. The photolysis rates were estimated using  $J_{\text{nitrate}}/J_{\text{NO}_2}$  ratios measured in this study and using  $J_{\text{NO}_2}$  for typical tropospheric irradiation conditions corresponding to the 1<sup>st</sup> July at noon and at 40° latitude North with (overhead ozone column 300, albedo 0.1; TUV NCAR Model, [http://www.cprm.acd.ucar.edu/Models/TUV/Interactive\\_TUV/](http://www.cprm.acd.ucar.edu/Models/TUV/Interactive_TUV/)). For  $J_{\text{NO}_2} = 1.03 \times 10^{-2} \text{ s}^{-1}$ , photolysis frequencies of carbonyl nitrates are:  $(6.1 \pm 0.9) \times 10^{-5} \text{ s}^{-1}$  for 4-nitrooxy-2-butanone and  $(3.3 \pm 0.9) \times 10^{-5} \text{ s}^{-1}$  for 5-nitrooxy-2-pentanone. Under these irradiation conditions, lifetimes ( $\tau_{\text{hv}} = 1/J$ ) were found to be 4 and 8 hours, respectively. For OH-oxidation, lifetimes ( $\tau_{\text{OH}} = 1/(k_{\text{OH}}[\text{OH}])$ ) were calculated using typical OH concentrations of  $2 \times 10^6 \text{ molecule cm}^{-3}$  (Atkinson and Arey, 2003). They are both equal to approximately two days. Hence, it appears that for 4-nitrooxy-2-butanone and for 5-nitrooxy-2-pentanone, photolysis is a more efficient sink than oxidation by OH radicals. An identical conclusion was obtained for  $\alpha$ -nitrooxy carbonyls (Suarez-Bertoa et al., 2012; Barnes et al., 1993; Zhu et al., 1991). However, OH-initiated oxidation is not negligible, especially under polluted conditions where OH concentrations can be higher than  $1 \times 10^7 \text{ molecule cm}^{-3}$ .

In order to evaluate the impact of these carbonyl nitrates on the nitrogen budget and the transport of NO<sub>x</sub>, it is crucial to determine whether their atmospheric sinks, here mainly photolysis, release NO<sub>2</sub> or not. For 4-nitrooxy-2-butanone, we observed that the photolysis proceeds mainly by a dissociation of the C(O)-C bond which does not necessarily lead to the release of NO<sub>2</sub> (see Scheme 2). In our experimental conditions (i.e., with high NO<sub>2</sub> mixing ratios), this pathway leads to the formation of PAN which was detected with a yield equal to unity. Under more realistic NO/NO<sub>2</sub> ratio, this reaction may also produce HCHO and CO<sub>2</sub>. The co-products of PAN, which could not be detected in our study, are expected to be formaldehyde + NO<sub>2</sub> or ethanal nitrate. One NO<sub>2</sub> molecule is hence released in the first hypothesis. Ethanal nitrate may react and undergo photolysis even faster than nitrooxy ketones and may thus lead to NO<sub>2</sub> release quite rapidly. However, as data on the reactivity of

ethanal nitrate are not available in the literature, one cannot provide a definite conclusion. In the case of 5-nitrooxy-2-pentanone, the dissociation of the C(O)-C bond has been observed to be a minor pathway suggesting that the major one, which was not directly observed here, is the O-NO<sub>2</sub> dissociation. This process certainly leads to the release of NO<sub>2</sub>.

#### 4 Conclusions

This paper presents the first study on the atmospheric reactivity of 4-nitrooxy-2-butanone and 5-nitrooxy-2-pentanone. Thanks to experiments in simulation chambers, photolysis frequencies and rate constants of the OH-oxidation were measured for the first time. From these results, it is concluded that, similarly to  $\alpha$ -nitrooxy ketones,  $\beta$ -nitrooxy ketones have enhanced UV absorption cross sections and quantum yields equal or close to unity, making photolysis a very efficient sink for these compounds. Results obtained for 5-nitrooxy-2-pentanone which is a  $\gamma$ -nitrooxy ketone, suggest a lower enhancement of cross sections leading to slightly longer atmospheric lifetimes. This can easily be explained by the increasing distance between the two chromophore groups. Some photolysis products were also detected allowing estimating the branching ratio between the two possible pathways, i.e., the dissociation of the C(O)-C bond and the one of the O-NO<sub>2</sub> bond. For 4-nitrooxy-2-butanone, we conclude that the photolysis proceeds mainly by a dissociation of the C(O)-C bond which does not necessarily lead to the release of NO<sub>2</sub>. In the case of 5-nitrooxy-2-pentanone, our results suggest that the dissociation of the O-NO<sub>2</sub> bond is the major pathway. Reactivity of 4-nitrooxy-2-butanone and 5-nitrooxy-2-pentanone with OH radicals was also investigated. Both compounds have similar reactivity towards OH radicals leading to lifetimes of approximatively two days. Experimental rate constants are in good agreement with those estimated by the SAR proposed by Kwok and Atkinson (1995) when using the parametrization proposed by Suarez-Bertoa et al. (2012) for carbonyl nitrates. However, this specific parametrization does not allow reproducing experimental data for monofunctional alkyl nitrates, suggesting that specific parametrization should be used for multifunctional species. Finally, these compounds are expected to be removed from the atmosphere fairly rapidly and to act as (only) temporary reservoirs of NO<sub>x</sub>. If formed during the night, they could however contribute to longer range transport of NO<sub>x</sub>.

#### 396 *Author contributions*

BPV coordinated the research project. BPV, RSB and JFD designed the experiments in simulation chambers. RSB performed the experiments with the technical support of MC and EP. RSB and MDa performed the organic syntheses. BPV, RSB and MDu performed the data treatment and interpretation. BPV and RSB wrote the paper and BPV was in charge of its final version. All coauthors revised the manuscript content, giving final approval of the version to be submitted.

#### 402 *Competing interests*

The authors declare that they have no conflict of interest.

#### 404 *Acknowledgments*

This work was supported by the French National Agency for Research (Project ONCEM-ANR-12-BS06-0017-01) and by the European Union within the 7th Framework Program, section “Support for Research Infrastructure-Integrated Infrastructure Initiative” through EUROCHAMP-2 project (RII3-CT-2009-228335) and the Horizon 2020 Research and Innovation Program through the EUROCHAMP-2020 Infrastructure Activity under grant agreement no. 730997. The authors thank Mila Ródenas ([mila@ceam.es](mailto:mila@ceam.es)) (CEAM, Paterna-Valencia, Spain) for the development and the free distribution of the software ANIR through the EUROCHAMP-2020 Data Centre website (<https://data.eurochamp.org>).

## References

- Atkinson, R., and Arey, J.: Gas-phase tropospheric chemistry of biogenic volatile organic compounds: a review, *Atmos. Environ.*, 37, 197-219, 2003.
- Barnes, I., Becker, K. H., and Zhu, T.: Near UV absorption spectra and photolysis products of difunctional organic nitrates: possible importance as NO<sub>x</sub> Reservoirs, *J. Atmos. Chem.*, 17, 353-373, 1993.
- Bean, J. K., and Hildebrand Ruiz, L.: Hydrolysis and gas-particle partitioning of organic nitrates formed from the oxidation of  $\alpha$ -pinene in environmental chamber experiments, *Atmos. Chem. Phys.* 15, 20629-20653, 2015.
- Beaver, M. R., St Clair, J. M., Paulot, F., Spencer, K. M., Crouse, J. D., LaFranchi, B. W., Min, K. E., Pusede, S. E., Wooldridge, P. J., Schade, G. W., Park, C., Cohen, R. C., and Wennberg, P. O.: Importance of biogenic precursors to the budget of organic nitrates: observations of multifunctional organic nitrates by CIMS and TD-LIF during BEARPEX 2009, *Atmos. Chem. Phys.*, 12, 5773-5785, 2012.
- Bedjanian, Y., Morin, J., and Romanias, M. N.: Reactions of OH radicals with 2-methyl-1-butyl, neopentyl and 1-hexyl nitrates. Structure-activity relationship for gas-phase reactions of OH with alkyl nitrates: An update, *Atmos. Environ.*, 180, 167-172, 2018.
- Clemishaw, K. C., Williams, J., Rattigan, O. V., Shallcross, D. E., Law, K. S., and Cox, R. A.: Gas-phase ultraviolet absorption cross-sections and atmospheric lifetimes of several C<sub>2</sub>-C<sub>5</sub> alkyl nitrates, *J. Photochem. Photobiol. A*, 102, 117-126, 1997.
- Doussin, J. F., Ritz, D., Durand-Jolibois, R., Monod, A., and Carlier, P.: Design of an environmental chamber for the study of atmospheric chemistry: New developments in the analytical device, *Analisis*, 25, 236-242, 1997.
- Duncanu, M., David, M., Kartigeyane, S., Cirtog, M., Doussin, J. F., and Picquet-Varrault, B.: Measurement of alkyl and multifunctional organic nitrates by Proton Transfer Reaction Mass Spectrometry, *Atmos. Meas. Tech.*, 10, 1445-1463, 2017.
- Finlayson-Pitts, B. J., and Pitts Jr., J. N.: *Chemistry of the Upper and Lower Atmosphere*, Academic Press, San Diego, 2000.
- Horowitz, L. W., Fiore, A. M., Milly, G. P., Cohen, R. C., Perring, A., Wooldridge, P. J., Hess, P. G., Emmons, L. K., and Lamarque, J.-F.: Observational constraints on the chemistry of isoprene nitrates over the eastern United States, *J. Geophys. Res.*, 112, D12S08, 2007.

Ito, A., Sillman, S., and Penner, J. E.: Effects of additional nonmethane volatile organic compounds, organic nitrates, and direct emissions of oxygenated organic species on global tropospheric chemistry, *Journal of Geophysical Research-Atmospheres*, 112, 10.1029/2005jd006556, 2007.

Jenkin, M. E., Valorso, R., Aumont, B., Rickard, A. R., and Wallington, T. J.: Estimation of rate coefficients and branching ratios for gas-phase reactions of OH with aliphatic organic compounds for use in automated mechanism construction, *Atmos. Chem. Phys.*, 18, 9297-9328, 10.5194/acp-18-9297-2018, 2018.

Kames, J., Schurath, U., Flocke, F., and Volz-Thomas, A.: Preparation of organic nitrates from alcohols and N<sub>2</sub>O<sub>5</sub> for species identification in atmospheric samples, *J. Atmos. Chem.*, 16, 349-359, 1993.

Kwok, E. S. C., and Atkinson, R.: Estimation of Hydroxyl Radical Reaction Rate Constants for Gas-Phase Organic Compounds using a Structure-Reactivity Relationship: an update, *Atmos. Environ.*, 29, 1685-1695, 1995.

Mao, J. Q., Paulot, F., Jacob, D. J., Cohen, R. C., Crouse, J. D., Wennberg, P. O., Keller, C. A., Hudman, R. C., Barkley, M. P., and Horowitz, L. W.: Ozone and organic nitrates over the eastern United States: Sensitivity to isoprene chemistry, *Journal of Geophysical Research-Atmospheres*, 118, 11256-11268, 10.1002/jgrd.50817, 2013.

Muller, J. F., Peeters, J., and Stavrakou, T.: Fast photolysis of carbonyl nitrates from isoprene, *Atmos. Chem. Phys.*, 14, 2497-2508, 10.5194/acp-14-2497-2014, 2014.

Neeb, P.: Structure-Reactivity Based Estimation of the Rate Constants for Hydroxyl Radical Reactions with Hydrocarbons, *J. Atmos. Chem.*, 35, 295-315, 2000.

Ng, N. L., Brown, S. S., Archibald, A. T., Atlas, E., Cohen, R. C., Crowley, J. N., Day, D. A., Donahue, N. M., Fry, J. L., Fuchs, H., Griffin, R. J., Guzman, M. I., Herrmann, H., Hodzic, A., Iinuma, Y., Jimenez, J. L., Kiendler-Scharr, A., Lee, B. H., Luecken, D. J., Mao, J. Q., McLaren, R., Mutzel, A., Osthoff, H. D., Ouyang, B., Picquet-Varrault, B., Platt, U., Pye, H. O. T., Rudich, Y., Schwantes, R. H., Shiraiwa, M., Stutz, J., Thornton, J. A., Tilgner, A., Williams, B. J., and Zaveri, R. A.: Nitrate radicals and biogenic volatile organic compounds: oxidation, mechanisms, and organic aerosol, *Atmos. Chem. Phys.*, 17, 2103-2162, 10.5194/acp-17-2103-2017, 2017.

Paulot, F., Crouse, J. D., Kjaergaard, H. G., Kroll, J. H., Seinfeld, J. H., and Wennberg, P. O.: Isoprene photooxidation: new insights into the production of acids and organic nitrates, *Atmos. Chem. Phys.*, 9, 1479-1501, 10.5194/acp-9-1479-2009, 2009.

Perring, A. E., Bertram, T. H., Farmer, D. K., Wooldridge, P. J., Dibb, J., Blake, N. J., Blake, D. R., Singh, H. B., Fuelberg, H., Diskin, G., Sachse, G., and Cohen, R. C.: The production and persistence of Sigma RONO<sub>2</sub> in the Mexico City plume, *Atmos. Chem. Phys.*, 10, 7215-7229, 10.5194/acp-10-7215-2010, 2010.

Perring, A. E., Pusede, S. E., and Cohen, R. C.: An Observational Perspective on the Atmospheric Impacts of Alkyl and Multifunctional Nitrates on Ozone and Secondary Organic Aerosol, *Chemical Reviews*, 113, 5848-5870, 10.1021/cr300520x, 2013.

Rindelaub, J. D., McAvey, K. M., and Shepson, P. B.: The photochemical production of organic nitrates from alpha-pinene and loss via acid-dependent particle phase hydrolysis, *Atmos. Environ.*, 100, 193-201, 10.1016/j.atmosenv.2014.10.010, 2015.

Roberts, J. M.: The Atmospheric Chemistry of organic Nitrates, *Atmos. Environ.*, 24A, 243-287, 1990.

484 Scarfogliero, M., Picquet-Varrault, B., Salce, J., Durand-Jolibois, R., and Doussin, J.-F.: Kinetic and  
Mechanistic Study of the Gas-Phase Reactions of a Series of Vinyl Ethers with the Nitrate Radical, *J.*  
486 *Phys. Chem. A*, 110, 11074-11081, 2006.

Squire, O. J., Archibald, A. T., Griffiths, P. T., Jenkin, M. E., Smith, D., and Pyle, J. A.: Influence of  
488 isoprene chemical mechanism on modelled changes in tropospheric ozone due to climate and land use  
over the 21st century, *Atmos. Chem. Phys.*, 15, 5123-5143, 10.5194/acp-15-5123-2015, 2015.

490 Suarez-Bertoa, R., Picquet-Varrault, B., Tamas, W., Pangui, E., and Doussin, J. F.: Atmospheric Fate of a  
Series of Carbonyl Nitrates: Photolysis Frequencies and OH-Oxidation Rate Constants, *Environ. Sci.*  
492 *Technol.*, 46, 12502-12509, 10.1021/es302613x, 2012.

Taylor, W. D., Allston, T. D., Moscato, M. J., Fazenkas, G. B., Koslowski, R., and Takacs, G. A.:  
494 Atmospheric Photodissociation lifetimes for nitromethane, methyl nitrite, and methyl nitrate., *Int. J.*  
*Chem. Kinet.*, 12, 231-240, 1980.

496 Turberg, M. P., Giolando, D. M., Tilt, C., Soper, T., Mason, S., Davies, M., Klingensmith, P., and  
Takacs, G. A.: Atmospheric Photochemistry of Alkyl Nitrates, *J. Photochem. Photobiol. A-Chem.*, 51,  
498 281-292, 1990.

Wang, J., Doussin, J. F., Perrier, S., Perraudin, E., Katrib, Y., Pangui, E., and Picquet-Varrault, B.:  
500 Design of a new multi-phase experimental simulation chamber for atmospheric photosmog, aerosol and  
cloud chemistry research, *Atmospheric Measurement Techniques*, 4, 2465-2494, 10.5194/amt-4-2465-  
502 2011, 2011.

Xiong, F. L. Z., Borca, C. H., Slipchenko, L. V., and Shepson, P. B.: Photochemical degradation of  
504 isoprene-derived 4,1-nitrooxy enal, *Atmos. Chem. Phys.*, 16, 5595-5610, 10.5194/acp-16-5595-2016,  
2016.

506 Zhu, T., Barnes, I., and Becker, K. H.: Relative-rate study of the gas-phase reaction of hydroxy radicals  
with difunctional organic nitrates at 298K and atmospheric pressure, *J. Atmos. Chem.*, 13, 301-311,  
508 1991.

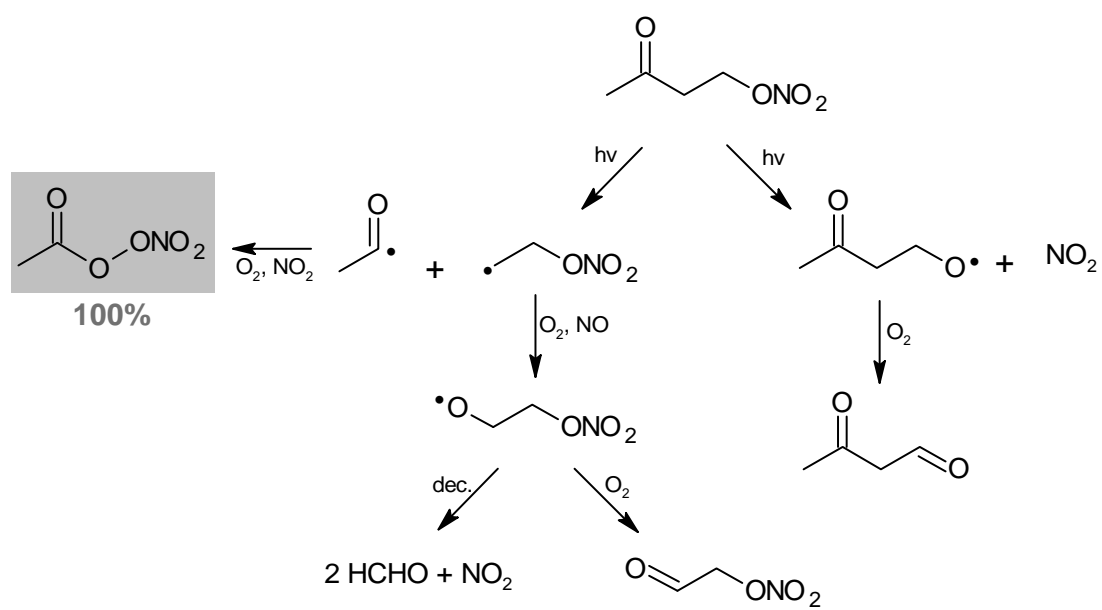
510

512

### Figure, scheme and table captions

- 514 **Scheme 1.** Photolysis pathways of 4-nitrooxy-2-butanone. Detected products are indicated with a grey background and their formation yield in given (in %).
- 516 **Scheme 2.** Photolysis pathways of 5-nitrooxy-2-pentanone. Detected products are indicated with a grey background and their formation yield in given (in %).
- 518 **Figure 1.** Kinetic plots for (a) the photolysis of 4-nitrooxy-2-butanone (experiment 2) and (b) the photolysis of 5-nitrooxy-2-pentanone (experiment 5). Red lines correspond to linear regressions.
- 520 **Figure 2.** Kinetic plots for the oxidation by OH radicals of 4-nitrooxy-2-butanone and 5-nitrooxy-2-pentanone. For 5-nitrooxy-2-pentanone, data have been shifted by 0.2 in y axis. Different symbols correspond to different
- 522 experiments.
- Table 1.** Photolysis rates and PAN yields for 4-nitrooxy-2-butanone and 5-nitrooxy-2-pentanone measured in
- 524 CESAM chamber.
- Table 2.** Comparison of experimental photolysis rates of carbonyl nitrates with those calculated for CESAM irradiation conditions and by assuming a quantum yield equal to unity.
- 526
- Table 3.** Rate constants for the OH-oxidation of 4-nitrooxy-2-butanone and 5-nitrooxy-2-pentanone.
- 528 **Table 4.** Comparison of experimental rate constants for the OH-oxidation of carbonyl nitrates with those estimated by SARs.
- 530 **Table 5.** Atmospheric lifetimes of carbonyl nitrates towards photolysis and reaction with OH radicals.

532

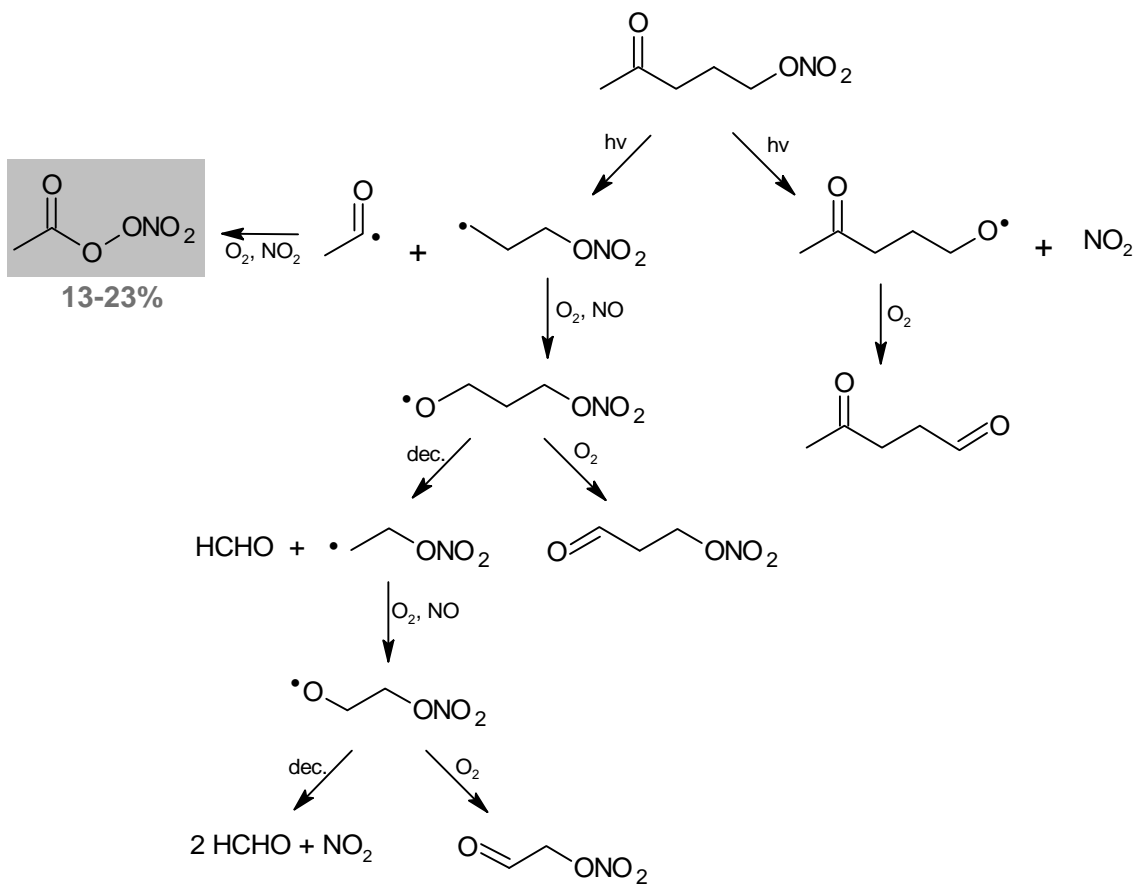


534

**Scheme 1.**

536





538 Scheme 2.

540

542

544

546

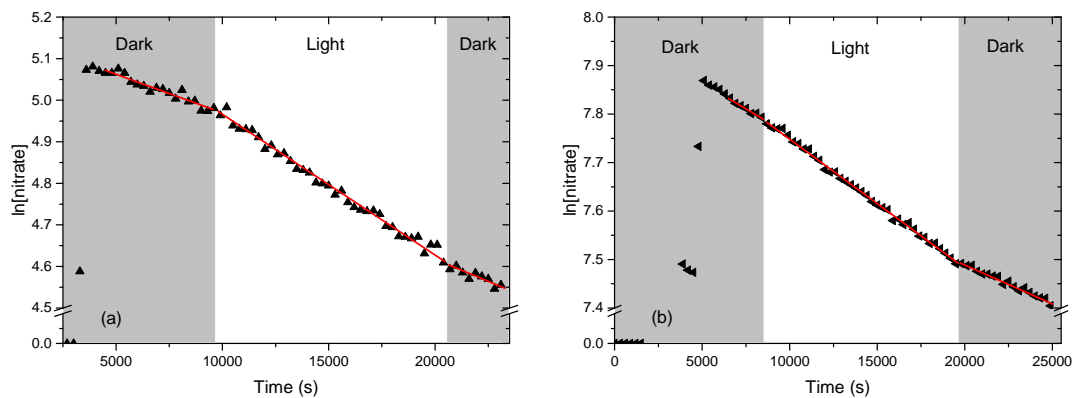
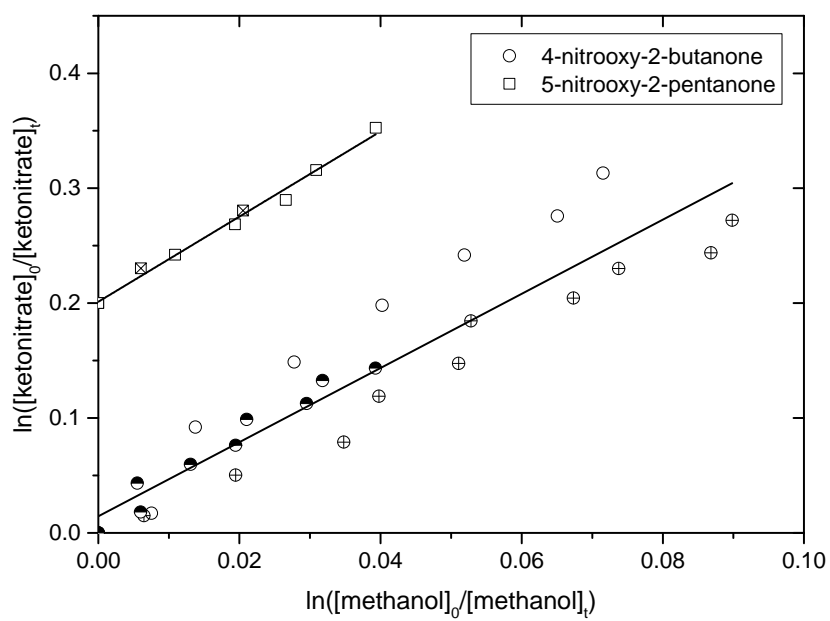


Figure 1.

548



550

Figure 2.

**Table 1.**

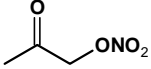
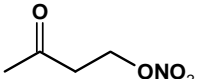
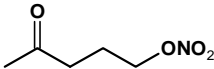
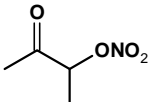
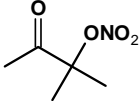
<b>Compound</b>	<b>Experim.</b>	$k_{\text{before}}^{\text{a}}$ ( $\times 10^{-5} \text{ s}^{-1}$ )	$k_{\text{after}}^{\text{b}}$ ( $\times 10^{-5} \text{ s}^{-1}$ )	$(k+J_{\text{nitrate}})^{\text{c}}$ ( $\times 10^{-5} \text{ s}^{-1}$ )	$J_{\text{nitrate}}^{\text{d}}$ ( $\times 10^{-5} \text{ s}^{-1}$ )	<b>PAN yield (%)</b>
4-nitrooxy-2- butanone	1	$0.8 \pm 0.1$	-	$2.1 \pm 0.1$	$1.3 \pm 0.2$	$100 \pm 35$
	2	$1.9 \pm 0.2$	$2.1 \pm 0.1$	$3.3 \pm 0.1$	$1.3 \pm 0.3$	$100 \pm 40$
	<b>Average</b>				<b><math>1.3 \pm 0.2</math></b>	<b><math>100 \pm 30</math></b>
5-nitrooxy-2- pentanone	3	$2.0 \pm 0.2$	$1.1 \pm 0.2$	$2.3 \pm 0.1$	$0.7 \pm 0.4$	$13 \pm 9$
	4	$1.9 \pm 0.2$	$1.1 \pm 0.1$	$2.2 \pm 0.1$	$0.7 \pm 0.4$	$13 \pm 9$
	5	$2.1 \pm 0.2$	$1.6 \pm 0.2$	$2.7 \pm 0.1$	$0.8 \pm 0.3$	$23 \pm 13$
	<b>Average</b>				<b><math>0.7 \pm 0.2</math></b>	<b><math>16 \pm 8</math></b>

552 <sup>a, b</sup> dark decay rate due to wall loss, before and after irradiation; <sup>c</sup> decay rate during irradiation  
554 period; <sup>d</sup> photolysis rate calculated as the difference between the decay rate during irradiation and  
the average dark decay rate.

556

558

560 **Table 2.**

Compound	$J_{\text{exp}} (\times 10^{-5} \text{ s}^{-1})$	$J_{\text{calc}} (\times 10^{-5} \text{ s}^{-1})$ ( $\phi=1$ )
<b>3-nitrooxy-2-propanone</b> 	$1.5 \pm 0.1$ (Suarez-Bertoa et al., 2012)	$1.4^{\text{b}}$
<b>4-nitrooxy-2-butanone</b> 	$1.3 \pm 0.2$ (This work)	$1.6^{\text{a}}$
<b>5-nitrooxy-2-pentanone</b> 	$0.7 \pm 0.2$ (This work)	$1.8^{\text{a}}$
<b>3-nitrooxy-2-butanone</b> 	$1.8 \pm 0.1$ (Suarez-Bertoa et al., 2012)	$2.2^{\text{b}}$
<b>3-methyl-3-nitrooxy-2-butanone</b> 	$2.31 \pm 0.05$ (Suarez-Bertoa et al., 2012)	ND

<sup>a</sup> calculated with estimated cross sections (see text); <sup>b</sup> calculated with experimental cross sections from literature;

562

**Table 3.**

<b>Compound</b>	$k_{\text{nitrate}}/k_{\text{methanol}}$	$k_{\text{nitrate}} \times 10^{-12}$ ( $\text{cm}^3 \text{ molecule}^{-1} \text{ s}^{-1}$ )
4-nitrooxy-2-butanone	$3.25 \pm 0.47$	$2.9 \pm 1.0$
5-nitrooxy-2-pentanone	$3.70 \pm 0.28$	$3.3 \pm 0.9$

564 **Table 4.**

Compound	$k_{\text{exp}}$ $\times 10^{-13}$	$k_{\text{SAR}}$ Atkinson/Bedjanian <sup>a</sup> $\times 10^{-13}$	$k_{\text{SAR}}$ Atkinson/Suarez <sup>b</sup> $\times 10^{-13}$	$k_{\text{SAR}}$ Neeb <sup>c</sup> $\times 10^{-13}$	$k_{\text{SAR}}$ Jenkin <sup>d</sup> $\times 10^{-13}$
3-nitrooxy-2-propanone	6.7 <sup>e</sup>	2.0	6.6	5.8	2.5
3-nitrooxy-2-butanone	10.1 <sup>e</sup>	4.5	13.2	6.8	3.7
3-methyl-3nitrooxy-2-butanone	2.6 <sup>e</sup>	4.0	2.1	2.4	4.3
4-nitrooxy-2-butanone	29 <sup>f</sup>	8.1	30.9	8.7	8.1
5-nitrooxy-2-pentanone	33 <sup>f</sup>	21.4	22.5	47.6	19.5

566 Rate constants are expressed in  $\text{cm}^3 \text{ molecule}^{-1} \text{ s}^{-1}$ ; <sup>a</sup> SAR developed by Kwok and Atkinson (1995) with F(-  
568  $\text{ONO}_2$ ) and F(-C- $\text{ONO}_2$ ) from Bedjanian et al., 2018; <sup>b</sup> SAR developed by Kwok and Atkinson (1995) with F(-  
 $\text{ONO}_2$ ) and F(-C- $\text{ONO}_2$ ) from Suarez-Bertoa et al., (2012) ; <sup>c</sup> SAR developed by Neeb (2000); <sup>d</sup> SAR developed  
by Jenkin et al. (2018) ; <sup>e</sup> experimental data from Suarez-Bertoa et al. (2012); <sup>f</sup> This work.

**Table 5.**

Compound	$J \times 10^{-5}$ <sup>a</sup> (s <sup>-1</sup> )	$\tau_{\text{hv}}$ (hours)	$k_{\text{OH}} \times 10^{-12}$ (cm <sup>3</sup> molecule <sup>-1</sup> s <sup>-1</sup> )	$\tau_{\text{OH}}$ <sup>b</sup> (hours)
4-nitrooxy-2-butanone	6.1 ± 0.9	4	2.9 ± 1.0	48
5-nitrooxy-2-pentanone	3.3 ± 0.9	8	3.3 ± 0.9	42

570 <sup>a</sup> photolysis frequencies estimated for a typical solar actinic flux (40°N, 1<sup>st</sup> July, noon) by applying a factor 4.7  
to those measured in CESAM chamber (see section 2.2); <sup>b</sup> estimated for [OH] = 2 × 10<sup>6</sup> molecule cm<sup>-3</sup>

572

574